




Original Article

Mechanobiology of Bone Consolidation During Distraction Osteogenesis: Bone Lengthening Vs. Bone Transport

PABLO BLÁZQUEZ-CARMONA ¹, JUAN MORA-MACÍAS,² JUAN MORGAZ,³
JOSÉ ANDRÉS FERNÁNDEZ-SARMIENTO,³ JAIME DOMÍNGUEZ,¹
and ESTHER REINA-ROMO¹

¹Escuela Técnica Superior de Ingeniería, Universidad de Sevilla, Avenida Camino de los Descubrimientos s/n, 41092 Seville, Spain; ²Escuela Técnica Superior de Ingeniería, Universidad de Huelva, 21007 Huelva, Spain; and ³Departamento Medicina y Cirugía Animal, Ctra. Nacional IV-A, Campus Universitario de Rabanales, Km 396, 14014 Córdoba, Spain

(Received 24 June 2020; accepted 16 October 2020)

Associate Editor Michael S. Detamore oversaw the review of this article.

Abstract—Bone lengthening and bone transport are regeneration processes that commonly rely on distraction osteogenesis, a widely accepted surgical procedure to deal with numerous bony pathologies. Despite the extensive study in the literature of the influence of biomechanical factors, a lack of knowledge about their mechanobiological differences prevents a clinical particularization. Bone lengthening treatments were performed on sheep metatarsus by reproducing the surgical and biomechanical protocol of previous bone transport experiments. Several *in vivo* monitoring techniques were employed to build an exhaustive comparison: gait analysis, radiographic and CT assessment, force measures through the fixation, or mechanical characterization of the new tissue. A significant initial loss of the bearing capacity, quantified by the ground reaction forces and the limb contact time with the ground, is suffered by the bone lengthening specimens. The potential effects of this anomaly on the musculoskeletal force distribution and the evolution of the bone callus elastic modulus over time are also analyzed. Imaging techniques also seem to reveal lower bone volume in the bone lengthening callus than in the bone transport one, but an equivalent mineralization rate. The simultaneous quantification of biological and mechanical parameters provides valuable information for the daily clinical routine and numerical tools development.

Keywords—Distraction osteogenesis, Gait analysis, *In vivo*, Stiffness monitoring, Bone consolidation, Callus volume.

Address correspondence to Pablo Blázquez-Carmona, Escuela Técnica Superior de Ingeniería, Universidad de Sevilla, Avenida Camino de los Descubrimientos s/n, 41092 Seville, Spain. Electronic mail: pbcarmona@us.es

INTRODUCTION

Callotaxis or distraction osteogenesis (DO) is a surgical technique that allows bone tissue to be generated between bony fragments.⁴⁷ As a clinical application of DO, bone lengthening (BL) has become an effective treatment for several bone pathologies, including limb length discrepancy or bone deformities.^{38,39,47} The standard treatment applies directly a gradual distraction to the bony fragments resulting from a single osteotomy until the clinically required elongation is achieved.⁴ Bone transport (BT) is another reconstructive approach based on DO to handle specific orthopedic diseases, such as non-unions or bone defects, especially infections.^{7,17,34,35} This technique is based on the progressive transport of a bony segment, normally osteotomized from the original bone, toward the infected/diseased bony fragment, which is generally removed in a surgery.^{7,9,34} Two main bone focuses are generated in this process at both sides of the transportable segment: the bone callus induced by distraction and the docking site.^{7,34} The main difference between BT and BL is the preservation of the limb's original length, avoiding potential problems derived from the elongation of the surrounding soft tissues.^{4,18,34}

One of the major limitations of these bone regeneration processes is the length of time required for the consolidation phase until the regenerated tissue is ossified and stabilized enough to disassemble the corresponding fixation.^{39,47} To prevent premature removal, daily clinical monitoring has traditionally been

based on qualitative techniques, including manual examinations or radiological evaluation of the callus bridging.^{14,40,54} Despite recent advances in the standardization of scoring systems,¹⁴ these data are generally not accurate enough by themselves to reach a safe decision.^{10,14,40,54} Lately, gait analysis has emerged as a complementary non-invasive approach to assess the evolution of a multitude of orthopedic pathologies.^{22,24,25,36,37} These studies cover kinetic parameters that are proven to be sensitive and consistent in evaluating functional changes.⁴¹ However, as far as the authors know, few previous studies have enquired into the relationship between the recovery of kinetic gait parameters and the consolidation of the immature tissue during DO.^{24,36,37}

For a more in-depth assessment of the tissue consolidation, diverse *ex vivo* strategies, such as nanoindentation^{26,28,30,32} or bending and torsion tests,¹⁵ provide spatial-temporal variations of the mechanical properties of the bone callus. However, these techniques mostly require the slaughter of the animal, and their standardization by correlations is highly limited by their dependence on the boundary conditions in which each mechanical test is performed. Computed tomography (CT) offers valuable information on the geometrical characteristics of the bone callus, as well as its mechanical properties.³ Nevertheless, reflections from the metallic components in the fixation prevent its application throughout the whole consolidation process.³⁵ As an alternative, *in vivo* monitoring techniques have recently arisen focusing on the temporal variation of mechanical parameters (force and strains through fixation, interfragmentary movements or accelerations after impact tests) as the new tissue mineralizes.^{9,20,29,33,35} Their main limitation is commonly related to the high dependence of their estimations on the stiffness of the corresponding fixation.⁸ The application of all these *in vivo* techniques extends the knowledge of DO processes and provides information for the development of numerical models for the *in silico* mechanical characterization of the callus as a future clinical tool.^{31,43–46,55}

Extensive literature has recognized the decisive role that several biomechanical factors play in bone regeneration processes.^{6,21,23,49} These factors, which affect the quantity and quality of new tissue, have been historically optimized in several DO applications to control the stress and strain distribution through the bone callus, which affect the quantity and quality of new tissue.⁵³ For instance, differences in the type of ossification (intramembranous or chondroid) due to alterations in the frequency and rate of distraction were reported in the literature²³ and its effects on tissue adaptation.¹ The impact of the latency period, the time from surgery until the beginning of distraction, on the

bone formation,²¹ or distraction forces⁴⁹ was also previously explored. Nevertheless, to our knowledge, no research has fixed all these biomechanical factors and gone into detail on the inter-differences between bone regeneration processes in mechanical terms, except for a few clinical studies based on the traditional assessing techniques.^{56,57}

This context of the broad diversity of monitoring techniques and biomechanical factors hinders a direct comparison between studies. In the literature, most research does not involve several measuring techniques for the analysis of multiple biomechanical parameters under a fixed distraction protocol, fixation system, and animal model. One exception is found in the BT studies of Mora-Macías *et al.*,^{30–36} which combine numerous *in vivo* and *ex vivo* approaches, resulting in an exhaustive characterization of the BT callus and its regeneration process using an unchanging experimental protocol and animal model. These BT studies, which form the basis of this work, have been reproduced in BL to look at the mechanobiological dissimilitude between both processes.

Therefore, the aim of this study is to analyze the evolution of several mechanical parameters during the consolidation of the BL callus, and compare them with the BT results reported by Mora-Macías *et al.*^{30–36} The differences in the evolution of kinetic and kinematics parameters from gait analysis were studied, as well as their possible relationship with the ossification of the resulting bone callus. This comparison was supplemented by quantifying *in vivo* the mechanical properties of the tissue through indirect non-invasive techniques, instrumented fixator, and CT images. This information could help in optimizing the clinical follow-up of each bone regeneration process and particularizing numerical models.

MATERIALS AND METHODS

Animals and Bone Lengthening Protocol

A BL treatment was performed on the right-back metatarsus of five skeletally-mature female Merino sheep, 2–4 years old, with a mean weight of 67.2 ± 4.9 kg. Animal Ethics of the University of Sevilla approved the study with these animals. Moreover, their welfare was guaranteed during surgical interventions and experimental phases following the European (2010/63/UE) and national (RD 1201/2005) regulations on animal experimentation, avoiding stressful situations, and providing analgesia during the procedure. The sheep were owned by the Research Center, the Hospital Clínico Veterinario of the University of Córdoba, where all *in vivo* experiments were carried

out, having first been purchased from a nearby farm. A metatarsus longer than 15 cm and wider than 10 mm was defined as an inclusion criterion to prevent surgical fractures in the fixation assembly. The animals were tested to ensure that they were not suffering from any parasitic or infectious diseases prior to their acquisition, and they were subsequently maintained. After the quarantine period, the animals remained in the research facility for 1–2 months to acclimatize and reduce stress before being included in the research.

During the course of the surgery, the animals were laid down in the right-lateral decubitus position with the limb to be operated resting on the surgical table. An Ilizarov-type external fixator, with an axial stiffness (K_F) of 593 ± 21 N/mm, was implanted to stabilize the resulting bony fragments in a mechanical environment equivalent to that used by Mora-Macías *et al.*^{33,35,36} The fixation consisted of two external frames attached to the bone using three Ø4 mm Schanz-pins per frame, inter-assembled by four fixed bars.⁵ After drilling the Schanz-pins and the fixation assembly, an osteotomy was performed in an intermediate cross-section of the metatarsus by means of a linear oscillating saw with a specific guide. The width of the blade was 1 mm, which prevented compressing or reducing the bony fragments after cutting. Details of the fixation and the osteotomy performed are displayed in Fig. 1a. The BT surgical protocol applied by Mora-Macías *et al.*^{33,35,36} was very similar, adapting the number of osteotomies until obtaining a transportable bony fragment through a 15 mm gap created after removing another bone segment, as shown in Fig. 1b. The anesthetic and postoperative protocols in both procedures were also similar. The animals were premedicated with dexmedetomidine (4 µg/kg) and morphine (0.2 mg/kg) intravenously through a cephalic vein. After 10 min of preoxygenation by mask, induction was performed with propofol, and their tracheas were intubated. The anesthetic was maintained with isoflurane and oxygen. After the surgery, the reanimation of the animals was controlled by the veterinarian team until the anesthesia effects had worn off. Finally, the sheep were monitored daily for potential infections around the fixation pins and received the same postoperative treatment of antibiotics (amoxicillin–clavulanic) and analgesia (buprenorphine and meloxicam).

The distraction osteogenesis protocol was also defined in accordance with the BT study carried out by Mora-Macías *et al.*^{33,35,36} Both protocols began with a latency period of seven days. After latency completion, the fixed bars were replaced with instrumented extendible bars,⁵ which allowed us to apply bony displacements in a controlled manner. In the course of the distraction phase, the bony fragments were gradually separated in the BL protocol, and the trans-

portable bony segment was moved until the original bone defect in the BT protocol was filled. In both cases, the rate and frequency of distraction were 1 mm/day, once a day for 15 days, resulting in a 15 mm bone callus. During the consolidation phase, walking tests were performed in a gait circuit to promote mechanical stimuli in the bone callus and to indirectly monitor its biomechanical evolution as detailed in the following subsection. Finally, the sheep were slaughtered at different time-points of the consolidation phase (Table 1) to carry out CT images of the bone callus at different ossification degrees.

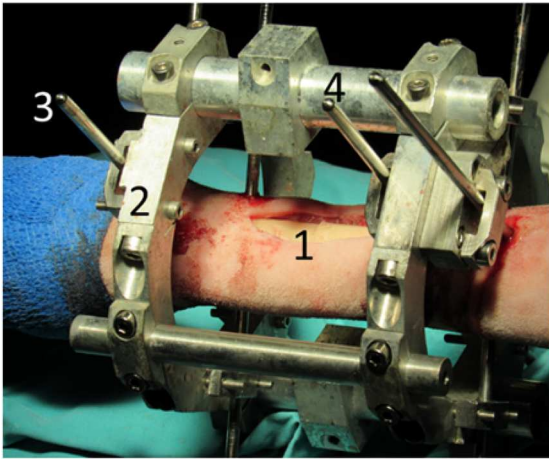
Measurement Devices and Data Collection

The bone regeneration evolution was indirectly monitored from the analysis of the data collected by several devices during walking tests, as illustrated in Fig. 2a. The bearing capacity in the operated limb, through the quantitative and qualitative progress of the ground reaction forces (GRF), and its contact time with the ground during the stance phase were analyzed using a load platform Pasco® PS-2141 (Pasco, Roseville, CA, EE.UU.). Two or three times a week, the sheep were led around a gait circuit, which included the instrumented walkway, wide enough for the animals to use their natural walking conditions. A minimum of 10 valid treads was measured every walking test, visually rejecting those in which the sheep did not reach a normal amble speed (2–4 km/h)^{11,35,36} or interrupted its walk at any point of the gait circuit.

The maximum ground reaction force (MGRF) of each walking test was determined as the average of the peak GRF values of each tread. This kinetic parameter was individually normalized by the bodyweight of each animal (% BW), and its evolution was studied as a clinical recovery index. Similarly, the daily contact time with the ground was defined as the mean value of the time invested in the validated treads. Moreover, a mean curve of three GRF individual curves (% BW) of a sheep during the stance phases of both operated ipsilateral hindlimb (HI) and non-operated ipsilateral forelimb (FI) was examined at three different time-points of the consolidation phase, weeks 3, 10 and 17 after surgery. Reference values of both MGRF values, contact time, and GRF curves were previously captured from a control group compounded by three non-treated animals.^{35,36}

The external fixator provided additional monitoring data. Their extendible bars, instrumented with four load cells Burster® 8431-6001 (Burster, Gernsbach, Germany), simultaneously quantified the force through the fixation (FF) during the treads of the sheep. Data was collected and wirelessly sent to a PC using a developed real-time and portable acquisition

BL



BT

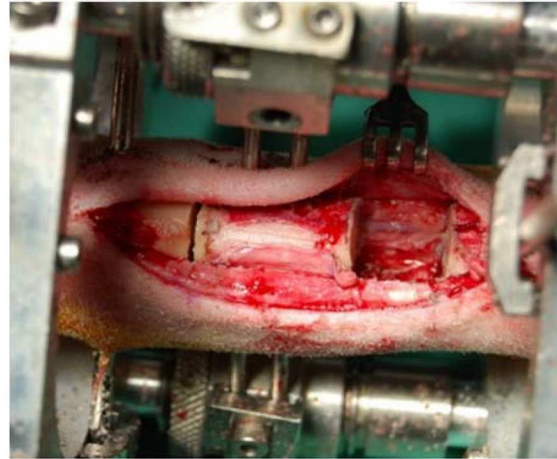


FIGURE 1. Images of the sheep right-metatarsus after performing the osteotomies in the course of the bone lengthening (BL) and bone transport (BT) surgeries: (1) osteotomy in an intermediate cross-section of the bone; (2) frames of the external fixator; (3) $\varnothing 4$ mm Schanz-pins; (4) non-instrumented fixed bars.

TABLE 1. Experimental information of each specimen: days from surgery until its slaughter, estimated length (L), and average area (\bar{A}) of the bone callus measured from the CT images for the estimation of the mechanical properties of the tissue over the time.

Sheep	Days from surgery	\bar{A} (mm ²)	L (mm)
1	161	373.93	14.45
2	112	391.15	13.97
3	64	346.04	12.91
4	29	274.24	12.67
5	18	270.26	12.93

system carried by the sheep during the walking tests.⁵ From these measures, the force distribution through the elongated limb and the mechanical properties of the bone callus can be estimated over the consolidation phase by applying the stiffness model specified in the subsequent subsection.

Model for Stiffness Estimation

A bone-fixator model for estimating the force distribution and the bone callus stiffness (K_{BC}) is presented in Fig. 2b. The voluntary gait motion of our specimens is produced by internal forces (IF), which traverses the musculoskeletal system of the limb. These internal forces are produced by the ground reaction and muscle forces.

During the distraction phase, the bone callus stiffness increases due to tissue maturation and the progressive orientation of the collagen fibers along the longitudinal axis.^{50,52} However, the peak stiffness val-

ues reported by Blázquez-Carmona *et al.*,⁴ between 18–23 N/mm in the first days of distraction, are negligible compared to the fixation stiffness ($K_{BC} \ll K_F$). Consequently, most of the IF goes through the external fixator ($FF \approx IF$), and the lower proportion through the bone callus could be neglected ($CF \approx 0$). As observed in previous studies,^{11,35} the IF/MGRF ratio was found to remain approximately constant in this early distraction stage. Its value 2.75 ± 0.40 was also assumed to be constant during the consolidation phase, presuming a constant proportion of IF invested in muscle activity during treads (IF/MF). Over time, the force through the callus (CF) increases as the tissue ossifies during the consolidation period. Once the IF is estimated from the GRF records, CF involved in a stance phase can be estimated at any time-point of the consolidation phase as:

$$CF = IF - FF = (2.75 \cdot MGRF) - FF \quad (1)$$

The K_{BC} was determined by assuming homogeneous mechanical properties of the bone callus. Applying the bone-fixator model (Fig. 2b), these stiffness values could be estimated from the IF distribution through the metatarsus and the stiffness of the external fixator (K_F). Finally, the apparent elastic modulus of the tissue (E_{BC}) can be characterized considering a length (L) and average cross-sectional area (\bar{A}) measured for each bone callus. These geometric parameters were calculated with the aid of CT images taken after the slaughter of the animal, and more details are described in the following subsection. Despite the changes in the percentage of mineralized volume reported by Mor-Macías *et al.*,^{31,35} this strategy is justified by the scarce

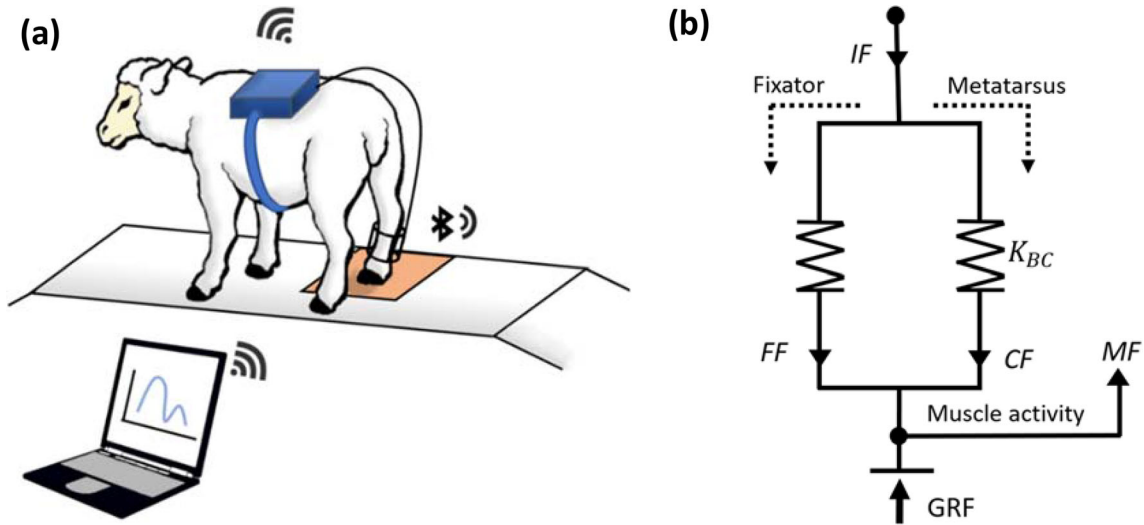


FIGURE 2. (a) Illustration of the measurement procedure during a walking test: (1) load platform embedded in the wooden walkway collecting and sending the GRF data; (2) instrumented external fixator implanted in the right-back metatarsus of the sheep; (3) acquisition system responsible for the collection and transmission of fixation force data (FF) to the PC; (4) PC receiving data in real-time. (b) Scheme of the forces distribution during a tread of a specimen: internal force (IF); forces through the external fixator (FF); stiffness of the fixation (K_F); forces through the bone callus (CF); stiffness of the bone callus (K_{BC}); ground reaction forces (GRF); force invested in the muscular activity (MF).

variation in the total volume of the bone callus (TV), bone volume (BV) plus non-mineralized soft tissue, during the consolidation phase, approximately the first 200 days after surgery. Therefore, the evolution of the mechanical properties of the bone callus during the consolidation phase was estimated as:

$$E_{BC} = K_{BC} \frac{L}{A} = K_F \frac{CF}{FF} \frac{L}{A} \quad (2)$$

Moreover, this model was validated *in vitro* in a previous work,⁵ simulating K_{BC} at different degrees of mineralization with wide-ranging elastic springs.

X-ray and CT Study of the Bone Callus

A radiographic follow-up was periodically performed during the distraction and consolidation phases to follow the separation of the bony fragments and qualitatively analyze the tissue consolidation, respectively.

Furthermore, CT images of the elongated limbs were taken *ex vivo* after the slaughter of each animal. The resolution of the images was 200–300 $\mu\text{m}/\text{voxel}$, and their manual segmentation was carried out using the medical software InVesalius® (Renato Archer Information Technology Center, Brazil), which employs the Hounsfield unit (HU) as a grayscale proportional to the density of the tissue. After the generation of three-dimensional models of the bone callus, their TV was estimated as well as their length, which was defined as the minimum distance between

cortical bony fragments. The average area of the cross-section of each bone callus was also determined as the quotient between the TV and the estimated length. The individualized values of these geometrical parameters are specified in Table 1. Finally, the BV and the % BV over the TV of each bone callus were also estimated by applying the predefined threshold HU values for bone tissue, 226–3071.

Statistical Analysis

The temporal evolution of the FF and CF has been modeled with logistic functions, as reported by other authors in literature,^{2,8,35} and fitted to the experimental data by the equation:

$$XF = \frac{0.5 \cdot \overline{IF}}{1 + e^{a(b+t)}} + \frac{0.5 \cdot \overline{IF}}{1 + e^{c(d+t)}} \quad (3)$$

where XF is the FF or the CF in % of the MGRF, \overline{IF} is the mean value of the IF, t is the day of the consolidation phase, and a , b , c and d are the fitting coefficients.

Besides, the evolution of the callus elastic modulus over the consolidation days was correlated with an exponential function also according to the behavior of the mechanical properties suggested in previous studies^{8,35}:

$$E = g \cdot e^{s \cdot t} \quad (4)$$

where E is Young Modulus of the bone callus in MPa, t is the day of the consolidation, g and s are the fitting coefficients.

The values of the fitting coefficients with the 95% confidence intervals (CI) of each correlation are specified in Tables 2 and 3, respectively. The determination coefficients (R^2 and p values) are also detailed, suggesting that the correlations were significant.

RESULTS

Gait Analysis and X-ray Control

The evolution of the bearing load of the limb of each specimen along with the consolidation phase, measured as the MGRF normalized by their individual BW, is shown in Fig. 3a (blue markers) with the BT results from Mora-Macías *et al.*³⁶ for further comparison. The mean MGRF of the control group (green dotted line) is also included, which was approximately 42–43% of the BW.³⁶ Sheep under BL treatment completed the distraction phase with significantly lower MGRF values than the control group, between 12.16 and 17.82% of the BW. Nevertheless, the bearing capacity of the elongated limb increased over the experimentation phase of each animal with a comparable recovering rate. The longest-term animal reached a MGRF of 38.38% of the BW after 119 days from the end of the distraction, similar values to healthy ones. Regarding the contact time with the ground during the stance phase of the operated HI limb, Fig. 3b shows the results obtained during the gait tests for the control group (green dotted line, 0.5973 s), BL group (blue points), and BT group for further discussion (red triangle markers). The BL animals initially presented a slightly shorter stance phase than the control group, mostly between 0.4 and 0.6 s. Nevertheless, they slowly improve their range of mobility until reaching contact time values similar to healthy ones from day 110.

Focusing on another kinematic parameter, GRF curves (% BW) during the stance phase of the sheep #1 under BL treatment are shown in Fig. 4 (blue data) along with the BT curves from Mora-Macías *et al.*³⁶ The tread of the FI limb is initially displayed, followed by the HI one. The evolution of the GRF curves was compared at the previously specified time-points: week 3, 11 and 17 after surgery. As a reference, the GRF curves obtained from the control group are also included in Fig. 4 (green curves). The present results concord with the previous findings of the bearing recovery: the GRF data of the operated limb began with levels substantially lower than healthy curves, but these differences decreased throughout the consolidation phase. According to Svodoba *et al.*,⁵¹ the gait

cycle of a healthy HI limb (Fig. 4, green curves) could be divided into four time-intervals based on the increasing and decreasing behavior of the GRF curve: loading response, midstance, terminal stance, and pre-swing. The evolution between subphases is mainly due to the contacts and take-offs between hoofs and ground and the fluctuation in the position of the body's center of gravity during the stance phase. In this context, the behavior of the HI curves is altered after distraction (Fig. 4, blue curves), losing the subphases mentioned above and the double GRF peaks in the medium-term. The FI limb presented an inverse evolution, slightly exceeding healthy values in the first days after distraction. This dissimilarity was progressively reduced as bone callus consolidates until presenting peak values equivalent to the control group (Fig 4, week 17). Nevertheless, the shapes of the FI curves were not identical either between BL and the control group at the time-points of the stance phase with the greatest load on the platform.

Radiographic images in the sagittal plane of the bone callus at the time-points analyzed are also shown in Fig. 5 (first row) together with BT images (second row). Focusing on BL, scarce soft tissue already closed the bridge between bony fragments at the end of the distraction phase (Fig. 5, BL week 3). The hypodense region decreased due to the callus tissue maturation and calcification but persisted in the weeks analyzed subsequently. Finally, a non-uniform ossification was observed, characterized by a faster consolidation in the posterior interzone (BL week 17).

Force Distribution and Callus Mechanical Properties

The distribution of forces through the skeletal structure of the elongated limb during treads is shown in Fig. 6a. These results were normalized by the MGRF in order to isolate the high dependency of the IF with the MGRF. The mean IF was represented (green line), being 2.75 MGRF. Most of the IF distributed to the external fixator (FF, blue curve) at the end of the distraction phase, around 2.5 MGRF. Nonetheless, the FF was gradually reducing over the consolidation phase coming to 0.37 MGRF after 80 days after surgery. At the same time, CF presented an inverse behavior, increasing from approximately 0.44 MGRF to 2.54 MGRF at the same time-point analyzed.

Regarding the mechanical properties of the new tissue, the elastic modulus of the bone callus also increased exponentially over time, as shown in Fig. 6b (blue line) together with BT evolution (red line). From values of between 0.03 and 10.85 MPa after distraction, the elastic modulus reached 139.50 MPa at day 75 from surgery.

TABLE 2. Fitting coefficients (Eq. 3) with their respective 95% confidence intervals and determination coefficients (R^2 and p value) of the fitting of the forces (% MGRF) through the external fixator (FF) and bone callus (CF) over time in days.

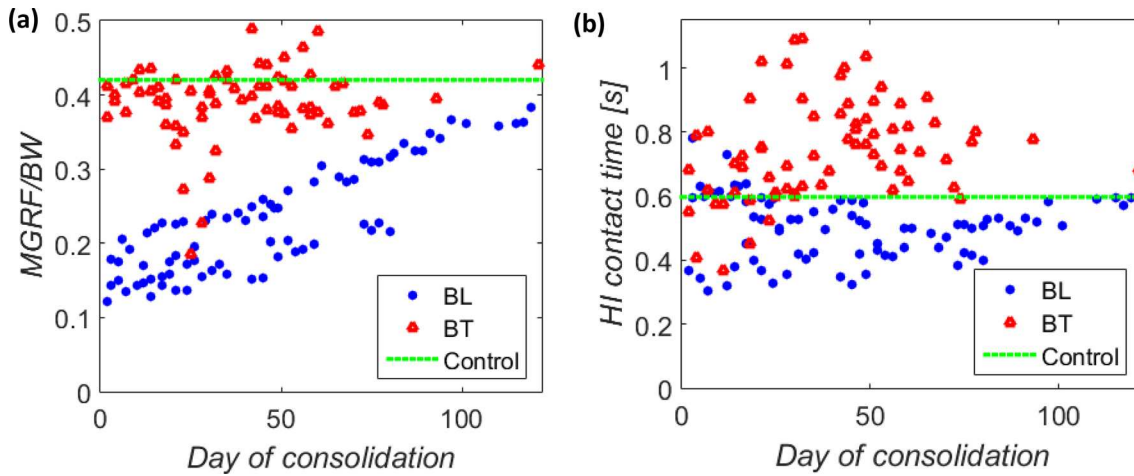
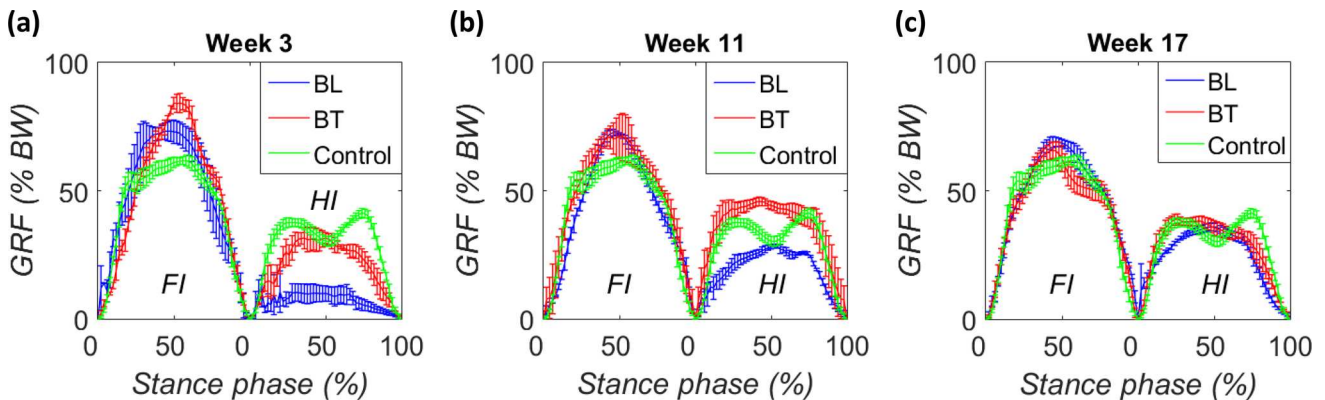
XF	a	b	c	d	R^2	p value
FF	0.15 ± 0.08	$- 27.95 \pm 9.78$	0.05 ± 0.04	$- 57.35 \pm 10.99$	0.85	< 0.001
CF	$- 0.15 \pm 0.08$	$- 34.28 \pm 8.07$	$- 0.04 \pm 0.03$	$- 55.63 \pm 12.33$	0.89	< 0.001

TABLE 3. Exponential coefficients with their respective 95% confidence intervals and determination coefficients (R^2 and p value) of the correlations corresponding to the evolution of the elastic modulus of the bone callus in MPa (Eq. 4).

Process	g	s	R^2	p value
BL	3.755 ± 1.473	0.048 ± 0.006	0.933	< 0.001
BT	8.754 ± 7.778	0.046 ± 0.033	0.642	< 0.001

Volume of the Bone Callus

The BV of each bone callus, measured at the slaughter time-points through the CT models, is shown in Fig. 7a with BT data³⁵ for further discussion. Besides, the volume of an original and untreated metatarsus fragment with an equivalent length, around 1.57 cm^3 , was additionally included as a reference. The BV strongly increased during the first days of consol-


FIGURE 3. (a) Evolution of the maximum ground reaction force (MGRF) normalized by the bodyweight of each specimen (BW) over the consolidation phase. (b) Evolution of the contact time with the ground invested by the operated ipsilateral hindlimb (HI) of the animals during a stance phase: BL sheep (blue points), BT data-points from Mora-Macias *et al.*³⁶ (red triangles), and mean value of the control group (dotted green line).

FIGURE 4. Evolution of the ground reaction force (GRF, % BW) during the stance phases of both non-operated ipsilateral forelimb (FI) and treated ipsilateral hindlimb (HI) in BL (blue), BT (red, from Mora-Macias *et al.*³⁶), and the control group (green). GRF curves are compared at three time-points after surgery: (a) week 3; (b) week 11; and (c) week 17.

idation until reaching a maximum value of 5.46 cm³ at day 112 after surgery. The degree of mineralization over the total volume (% BV over TV) is also presented in Fig. 7b. The BL calluses present fast mineralization during the first days of the consolidation phase, reaching 88.18–93.97 % of BV at days 121–161 after surgery.

DISCUSSION

The results presented in this experimental BL study reveal important findings in the understanding of the DO treatments. Several analyses were simultaneously carried out to investigate the mechanobiological differences and similarities with BT, as well as providing helpful clinical information.

Our specimens suffered a predictable lameness because of the surgery and the limb length increase produced by the distraction phase, reflected in their MGRF values and HI contact time during the stance phase (Fig. 3, blue markers). Regarding the MGRF parameter, when comparing this DO process to the BT result³⁶ (Fig. 3a, red markers), the gait disorder in BL becomes much more remarkable. BT animals hardly manifested loss of bearing capacity, starting the consolidation phase with MGRF values, approximately 37–42% of the BW, considerably close to the control group, 42% of the BW. In contrast, a stronger initial lameness in BL led to a slower recovery that was not complete after 120 days of consolidation. An intermediate result was obtained in the fracture healing study of Seebeck *et al.*⁴⁸ They reported a minimum MGRF value of approximately 29% of BW after distracting a tibiae sheep osteotomy to a 3 mm gap. Concerning the HI contact time, the prolonged reduction in mobility of the elongated limb contrasts with the rapid recovery in BT sheep (Fig. 3b, red triangles) up to the control values from day 30 of consolidation, 0.4–0.8 s. The subsequent slowdown in the BT stance phase could be due to the weight of the external fixator. This kinematic parameter normalizes in the medium-term in both bone regeneration processes. The mineralization process of the BT group seems to have a low impact on the analyzed parameters (MGRF and HI). Concerning the BL group, discomfort derived from distraction in long bones is suggested to be a significant factor in the gait disturbances, which has been shown to persist during the consolidation phase and restrain functional weight-bearing.^{20,58} This side effect could gain significance with the elongation percentage, about 12.5% of the original bony length in our study, which intensifies the damages caused by the stretching of the surrounding soft tissues,^{4,20,39} and a lowering of the nerve conductivity.¹⁸ Functional limb

length discrepancy could also induce temporal deformities according to literature,^{20,37} which could affect the loading capacity of the treated limb up to the development of compensation mechanics. In particular, limb deformity was visually manifested in our specimens by a rotation in the sagittal plane of the hoof, as reported in Blázquez-Carmona *et al.*⁴

Regardless of the dissimilarities in the MGRF values in the HI limb, BL (blue curves) and BT (red curves) treatments seem to share a similar pattern in the GRF shape to the control data (green data), as shown in Fig. 4. The disappearance of the second maximum peak, corresponding to the gait propulsion between terminal stance and pre-swing subphases in a healthy gait cycle, is a pattern shared between both bone regeneration processes. Moreover, this effect is also in accordance with the BL studies of Morasiewicz *et al.*³⁷ in humans, which attributed it to a weakening of the plantar flexor. Meanwhile, FI limb initially acquires a higher bearing load during gait in both DO processes as a compensatory mechanism to the bearing deficit of the HI limb, which is normalizing throughout the consolidation phase. This load redistribution ties well with previous studies in other animal models, e.g. the study in dogs with lameness of Fischer *et al.*¹³

The force distribution through the HI limb presented a high dependence of the IF on the loss of the bearing capacity suffered by our specimens. Deleting this dependency with a MGRF normalization according to the data presented in Fig. 6a, the CF and FF preserve their symmetric evolution as reported in BL processes by Mora-Macías *et al.*³⁵ Also, the recovery rate of the CF is practically identical in both bone regeneration processes, 80–90% of the IF after 50 days of consolidation. In tibia sheep, Grasa *et al.*¹⁹ reported in fracture healing this recovery level after approximately 30 days of consolidation. Meanwhile, 200 days of consolidation were required by Aarnes *et al.*² for an average of 31 mm lengthening in human tibiae.

From the imaging techniques, some biological conclusions can also be drawn. Comparing the BL and BT radiographic planes (Fig. 5) at the same weeks after surgery, the reported non-uniformity in the density scale between BL callus regions disappears in BT, and is not repeated in other BL studies in sheep tibiae.^{16,42} This effect could be related to a non-homogeneous force distribution in the bony cross-section caused by the compensatory gait mechanism after elongation or by a non-uniform cross-sectional stiffness distribution of the surrounding soft tissues. On the other hand, the volume of the bone callus seems to be higher in BT. Some previous conclusions can be supported by the CT analysis (Fig. 7). Despite sharing a similar tendency, reaching the maximum bone volume

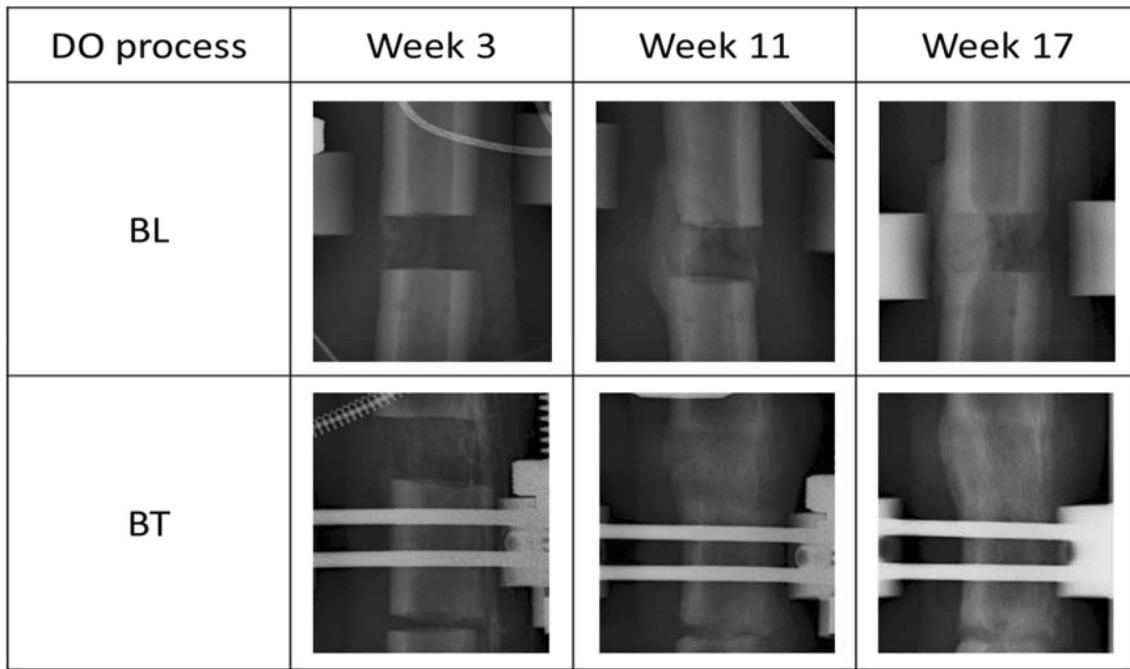


FIGURE 5. X-ray images of the BL (first row) and BT (second row) bone callus at three time-points of the consolidation phase: week 3, week 11 and week 17 after surgery.

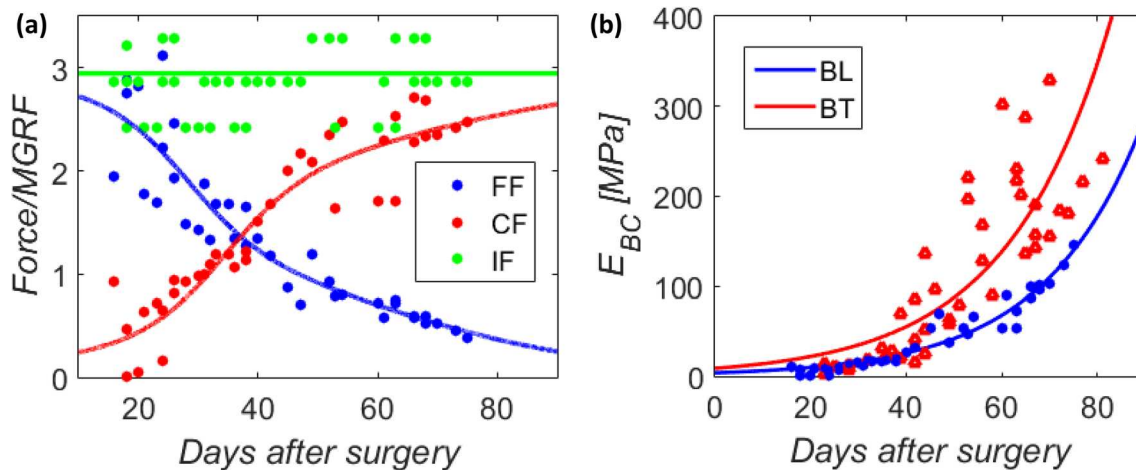


FIGURE 6. (a) Distribution of the internal force (IF, green) through the external fixator (FF, blue markers) and bone callus (CF, red markers) normalized by the maximum ground reaction force (MGRF) over the days after surgery. Markers represent the experimental points and the continuous lines represents the mean value (IF) and correlations (FF and CF), respectively. (b) Evolution of the elastic modulus of the bone callus over the days from surgery during two bone regeneration processes: BL (blue points) and BT (red triangles, from Mora-Macías *et al.*³⁵). Markers represent the experimental points, and continuous line the corresponding correlation.

after approximately 121 days after surgery, the BV increase of the BL callus (Fig. 7a, blue bars) could be slightly lower than the BT one (Fig. 7a, red bars) obtained in BT by Mora-Macías *et al.*³⁵ Furthermore, the BV of both processes remains above the control group (Fig. 7a, green bars), 1.57 cm^3 , in this phase prior to bone remodeling. Nevertheless, the mineralization rate (Fig. 7b) is equivalent between BL (blue

points) and BT³¹ (red triangles) processes: 88.18–93.97 % and 87.55–100 % of BV at days 121–161, respectively. These results validate some conclusions obtained from the gait analysis: the rate of consolidation is not a sole cause of the greater lameness of the BL group and their slow recovery, but also the surrounding soft tissue damage and the limb length discrepancy. Moreover, the suggested higher BV values in

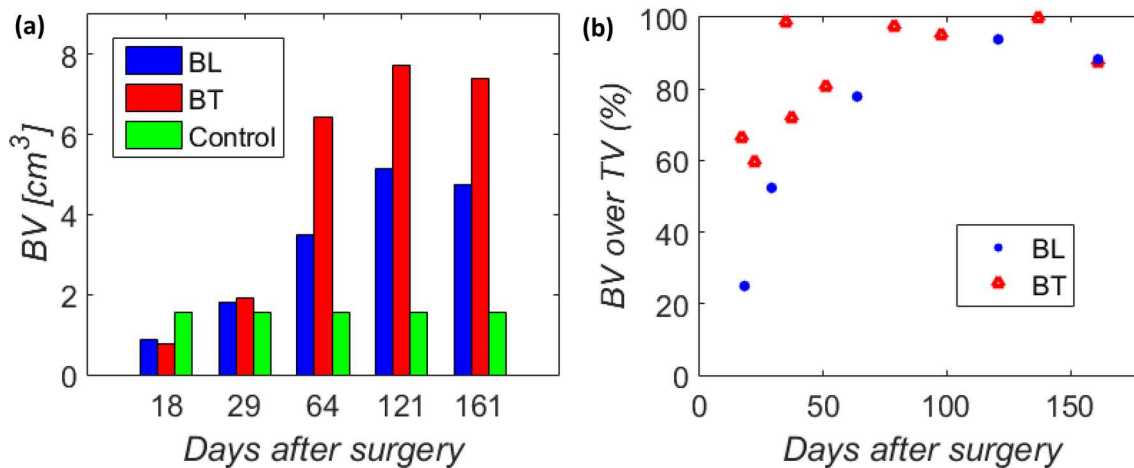


FIGURE 7. (a) Bone volume of bone callus (BV) at different time-points after surgery, estimated after the segmentation of CT images during two bone regeneration processes: BL (blue bars), BT (red bars from the correlation of Mora-Macias *et al.*³⁵), and control sheep (green bars). (b) Evolution of the % BV over total callus volume (TV) through the days after surgery in both processes: BL (blue points) and BT from Mora-Macias *et al.*³¹ (red triangles).

BT and the similar mineralization rates could indicate a higher TV in the BT callus, as observed in the x-ray analysis. As far as the authors know, no other previous study has radiologically compared the consolidation of bone callus from both bone regeneration processes with the same surgery protocol and biomechanical factors.

Focusing on the mechanical characterization of the bone callus, the evolution of the elastic modulus in the BL callus (Fig. 6b, blue data) and BT ones from Mora-Macias *et al.*³⁵ (red data) reveals interesting findings. Fitting correlation, determination coefficients and confidence intervals of the BT fitting are specified in Table 3. Moreover, the Pearson correlation coefficient between both correlation curves, being 0.9646. This parameter suggests that the evolutions of the mechanical properties are statistically similar between both bone calluses during the consolidation phase. However, the elastic modulus of the BT callus seems to experience a slightly more exponential increase from 8.75 to 347.10 MPa in 80 days, vs. a BL increase from 3.76 to 177.51 MPa. This non-simultaneous ossification is consistent with the degree of mineralization perceived on the radiographic images based on their grayscale (Fig. 5). Given the similarities in mineralization rates between bone regeneration processes presented in Fig. 7b, a lower woven bone maturation rate derived from a lower mechanical stimulation in the BL callus, previously quantified with the MGRF values, could be a possible explanation for this difference. The nanoindentation study of Mora-Macias *et al.*³² in sheep metatarsus also reported a wide range of variation of the woven bone elastic modulus in different bone calluses, from 7 to 14 GPa between days 35 and 525 after surgery, which is 77% of the estimated

value for cortical bone. The order of magnitude of our results also agrees with the elastic modulus measured in rat fracture callus *via* nanoindentation by Leong and Morgan,^{26,27} around 27–1010 MPa. Finally, the exponential recovery behavior of the mechanical properties in the distraction callus agrees also with previous studies in literature.^{12,35}

Before concluding the discussion, it is important to point out some limitations of this study, especially in relation to the mechanical characterization of callus. A homogeneous behavior was assumed throughout the complete bone callus due to the *in vivo* indirect assessment. This procedure prevents inquiring into the ossification differences between callus inter-zones observed in the X-ray images. Furthermore, the callus dimensions for the elastic modulus estimation were fixed from the CT images after the slaughter of each animal, neglecting its slight evolution during the consolidation phase. Reflections from the metallic components of the external fixator avoid a more weekly monitoring of the volume evolution over time. Finally, the number of specimens is another limitation that prevents drawing more exhaustive conclusions.

Our results demonstrate a possible slower rate of ossification in BL callus than BT ones, possibly derived from gait compensation mechanisms and the loss of bearing capacity quantified by the MGRF. The gait of the operated limb after distraction is more altered in BL due to the damage caused to the surrounding soft tissues. Radiological monitoring also suggests a more uniform load distribution in the BT callus. These conclusions are reinforced by the extensive direct comparison between studies that share bone model and biomechanical factors. All multidisciplinary provided information allows a better experimental understand-

ing of DO processes combining biological and mechanical data, which may be of interest in developing numerical tools as a future clinical resource.

ACKNOWLEDGMENTS

We thank the Junta de Andalucía and the Ministerio de Economía y Competitividad from the Government of Spain for funding this research (US-1261691, DPI2017-82501-P, and PGC2018-097257-B-C31) and the FPU Grant of one of the authors (FPU17/05361).

CONFLICT OF INTEREST

The authors have no financial or personal relationships which could inappropriately influence the contents of this paper. Therefore, no conflict of interest is declared.

REFERENCES

- ¹Aarnes, G. T., H. Steen, P. Ludvigsen, L. P. Kristiansen, and O. Reikerås. High frequency distraction improves tissue adaptation during leg lengthening in humans. *J Orthop. Res.* 20:789–792, 2002.
- ²Aarnes, G. T., H. Steen, P. Ludvigsen, N. A. Waanders, R. Huijskes, and S. A. Goldstein. In vivo assessment of regenerate axial stiffness in distraction osteogenesis. *J. Orthop. Res.* 23:494–498, 2005.
- ³Augat, P., E. F. Morgan, T. J. Lujan, T. J. MacGillivray, and W. H. Cheung. Imaging techniques for the assessment of fracture repair. *Injury.* 45(Suppl 2):S16–S22, 2014.
- ⁴Blázquez-Carmona, P., J. Mora-Macías, J. A. Sanz-Herrera, J. Morgaz, R. Navarrete-Calvo, J. Domínguez, and E. Reina-Romo. Mechanical influence of surrounding soft tissue on bone regeneration processes: a bone lengthening study. *Ann. Biomed. Eng.* 2020. <https://doi.org/10.1007/s10439-020-02592-z>.
- ⁵Blázquez-Carmona, P., M. Sanchez-Raya, J. Mora-Macías, J. A. Gómez-Galán, J. Domínguez, and E. Reina-Romo. Real-time wireless platform for in vivo monitoring of bone regeneration. *Sensors.* 20:4591, 2020.
- ⁶Breik, O., D. Tivey, K. Umaphathysivam, and P. Anderson. Does the rate of distraction or type of distractor affect the outcome of mandibular distraction in children with micrognathia? *J. Oral Maxillofac. Surg.* 74:1441–1453, 2016.
- ⁷Brunner, U. H., J. Cordey, L. Schweiberer, and S. M. Perren. Force required for bone segment transport in the treatment of large bone defects using medullary nail fixation. *Clin. Orthop. Relat. Res.* 301:147–155, 1994.
- ⁸Claes, L. E., and J. L. Cunningham. Monitoring the mechanical properties of healing bone. *Clin. Orthop. Relat. Res.* 467:1964–1971, 2009.
- ⁹Claes, L., J. Laule, K. Wenger, G. Suger, U. Liener, and L. Kinzl. The influence of the fixator on maturation of the callus after segmental transport. *J. Bone Joint Surg. Br.* 82:142–148, 2000.
- ¹⁰Corrales, L. A., S. Morshed, M. Bhandari, and T. Miclau, III. Variability in the assessment of fracture-healing in orthopaedic trauma studies. *J. Bone Joint Surg. Am.* 90:1862–1868, 2008.
- ¹¹Duda, G. N., K. Eckert-Hübner, R. Sokiranski, A. Kreutner, R. Miller, and L. Claes. Analysis of inter-fragmentary movement as a function of musculoskeletal loading conditions in sheep. *J. Biomech.* 31:201–210, 1998.
- ¹²Dwyer, J. S., P. J. Owen, G. A. Evans, J. H. Kuiper, and J. B. Richardson. Stiffness measurements to assess healing during leg lengthening. A preliminary report. *J. Bone Joint Surg. Br.* 78:286–289, 1996.
- ¹³Fischer, S., A. Anders, I. Nolte, and N. Schilling. Compensatory load redistribution in walking and trotting dogs with hind limb lameness. *Vet. J.* 197:746–752, 2013.
- ¹⁴Fisher, J. S., J. J. Kazam, D. Fufa, and R. J. Bartolotta. Radiologic evaluation of fracture healing. *Skeletal Radiol.* 48:349–361, 2019.
- ¹⁵Floerkemeier, T., F. Thorey, C. Hurschler, M. Wellmann, F. Witte, and H. Windhagen. Stiffness of callus tissue during distraction osteogenesis. *Orthop. Traumatol. Surg. Res.* 96:155–160, 2010.
- ¹⁶Forriol, F., L. Denaro, U. G. Longo, H. Taira, N. Maffulli, and V. Denaro. Bone lengthening osteogenesis, a combination of intramembranous and endochondral ossification: an experimental study in sheep. *Strategies Trauma Limb Reconstr.* 5:71–78, 2010.
- ¹⁷Fürmetz, J., C. Soo, W. Behrendt, P. H. Thaller, H. Siekmann, J. Böhme, and C. Josten. Bone transport for limb reconstruction following severe tibial fractures. *Orthop. Rev.* 8:6384, 2016.
- ¹⁸Galardi, G., G. Comi, L. Lozza, P. Marchettini, M. Novarina, R. Facchini, and A. Paronzini. Peripheral nerve damage during limb lengthening. Neurophysiology in five cases of bilateral tibial lengthening. *J. Bone Jt Surg. Br.* 72:121–124, 1990.
- ¹⁹Grasa, J., M. J. Gómez-Benito, L. A. González-Torres, D. Asiain, F. Quero, and J. M. García-Aznar. Monitoring in vivo load transmission through an external fixator. *Ann. Biomed. Eng.* 38:605–612, 2010.
- ²⁰Hasler, C. C., and A. H. Krieg. Current concepts of leg lengthening. *J. Child. Orthop.* 6:89–104, 2012.
- ²¹Hayashi, K., I. Yoshioka, A. Khanal, N. Furuta, K. Tomimaga, and J. Fukuda. Effects of latency on bone formation during consolidation period of rabbit mandibular distraction. *Asian J. Oral Maxillofac. Surg.* 20:5–11, 2008.
- ²²Jacobs, B. Y., H. E. Kloeffkorn, and K. D. Allen. Gait analysis methods for rodent models of osteoarthritis. *Curr. Pain Headache Rep.* 18:456, 2014.
- ²³Kessler, P., F. W. Neukam, and J. Wiltfang. Effects of distraction forces and frequency of distraction on bony regeneration. *Br. J. Oral. Maxillofac. Surg.* 43:392–398, 2005.
- ²⁴Koczewski, P., F. Urban, and M. Józwiak. Analysis of some gait parameters at different stages of leg lengthening using the Ilizarov technique. *Chir Narzadow Ruchu Orthop. Pol.* 69:393–397, 2004.
- ²⁵Krizsan-Agbas, D., M. K. Winter, L. S. Eggimann, J. Meriwether, N. E. Berman, P. G. Smith, and K. E.

- McCarson. Gait analysis at multiple speeds reveals differential functional and structural outcomes in response to graded spinal cord injury. *J. Neurotrauma*. 31:846–856, 2014.
- ²⁶Leong, P. L., and E. F. Morgan. Measurement of fracture callus material properties via nanoindentation. *Acta Biomater*. 4:1569–1575, 2008.
- ²⁷Leong, P. L., and E. F. Morgan. Correlations between indentation modulus and mineral density in bone-fracture calluses. *Integr. Comp. Biol*. 49:59–68, 2009.
- ²⁸Manjubala, I., Y. Liu, D. R. Epari, P. Roschger, H. Schell, P. Fratzl, and G. N. Duda. Spatial and temporal variations of mechanical properties and mineral content of the external callus during bone healing. *Bone*. 45:185–192, 2009.
- ²⁹Mattei, L., F. Di Puccio, and S. Marchetti. In vivo impact testing on a lengthened femur with external fixation: a future option for non-invasive monitoring of fracture healing? *J. R. Soc. Interface*. 15:20180068, 2018.
- ³⁰Mora-Macías, J., P. García-Florencio, A. Pajares, P. Miranda, J. Domínguez, and E. Reina-Romo. Elastic modulus of woven bone: correlation with evolution of porosity and x-ray greyscale. *Ann. Biomed. Eng.* 2020. <https://doi.org/10.1007/s10439-020-02529-6>.
- ³¹Mora-Macías, J., M. A. Giráldez-Sánchez, M. López, J. Domínguez, and M. E. Reina-Romo. Comparison of methods for assigning the material properties of distraction callus in computational model. *Int. J. Numer. Method. Biomed. Eng.* 35:e3227, 2019.
- ³²Mora-Macías, J., A. Pajares, P. Miranda, J. Domínguez, and E. Reina-Romo. Mechanical characterization via nanoindentation of the woven bone developed during bone transport. *J. Mech. Behav. Biomed. Mater.* 74:236–244, 2017.
- ³³Mora-Macías, J., E. Reina-Romo, and J. Domínguez. Distraction osteogenesis device to estimate the axial stiffness of the callus in vivo. *Med. Eng. Phys.* 37:969–978, 2015.
- ³⁴Mora-Macías, J., E. Reina-Romo, and J. Domínguez. Model of the distraction callus tissue behavior during bone transport based in experiments in vivo. *J. Mech. Behav. Biomed. Mater.* 61:419–430, 2016.
- ³⁵Mora-Macías, J., E. Reina-Romo, M. López-Pliego, M. A. Giráldez-Sánchez, and J. Domínguez. In vivo mechanical characterization of the distraction callus during bone consolidation. *Ann. Biomed. Eng.* 43:2663–2674, 2015.
- ³⁶Mora-Macías, J., E. Reina-Romo, J. Morgaz, and J. Domínguez. In vivo gait analysis during bone transport. *Ann. Biomed. Eng.* 43:2090–2100, 2015.
- ³⁷Morasiewicz, M., P. Koprowski, Z. Wrzosek, and S. Dragan. Gait analysis in patients after lengthening and correction of tibia with Ilizarov technique. *Physiotherapy*. 18:9–18, 2010.
- ³⁸Moseley, C. F. Leg lengthening. A review of 30 years. *Clin. Orthop. Relat. Res.* 247:38–43, 1989.
- ³⁹Paley, D. Problems, obstacles, and complications of limb lengthening by Ilizarov technique. *Clin. Orthop. Relat. Res.* 250:81–104, 1990.
- ⁴⁰Panjabi, M. M., S. D. Walter, M. Karuda, A. A. White, and J. P. Lawson. Correlations of radiographic analysis of healing fractures with strength: a statistical analysis of experimental osteotomies. *J. Orthop. Res.* 3:212–218, 1985.
- ⁴¹Pardes, A., B. R. Freedman, and L. J. Soslowsky. Ground reaction forces are more sensitive gait measures than temporal parameters in rodents following rotator cuff injury. *J. Biomech.* 49:376–381, 2016.
- ⁴²Reichel, H., S. Lebek, C. Alter, and W. Hein. Biomechanical and densitometric bone properties after callus distraction in sheep. *Clin. Orthop. Relat. Res.* 357:237–254, 1998.
- ⁴³Reina-Romo, E., M. J. Gómez-Benito, J. M. García-Aznar, J. Domínguez, and M. Doblaré. Modeling distraction osteogenesis: analysis of the distraction rate. *Biomech. Model Mechanobiol.* 8:323–335, 2009.
- ⁴⁴Reina-Romo, E., M. J. Gómez-Benito, J. M. García-Aznar, J. Domínguez, and M. Doblaré. An interspecies computational study on limb lengthening. *Proc. Inst. Mech. Eng.* 224:1245–1256, 2010.
- ⁴⁵Reina-Romo, E., M. J. Gómez-Benito, J. M. García-Aznar, J. Domínguez, and M. Doblaré. Growth mixture model of distraction osteogenesis: effect of pre-traction stresses. *Biomech. Model Mechanobiol.* 9:103–115, 2010.
- ⁴⁶Reina-Romo, E., M. J. Gómez-Benito, A. Sampietro-Fuentes, J. Domínguez, and J. M. García-Aznar. Three-dimensional simulation of mandibular distraction osteogenesis: mechanobiological analysis. *Ann. Biomed. Eng.* 39:35–43, 2011.
- ⁴⁷Sailhan, F. Bone lengthening (distraction osteogenesis): a literature review. *Osteoporos. Int.* 22:2011–2015, 2011.
- ⁴⁸Seebeck, P., M. S. Thompson, A. Parwani, W. R. Taylor, H. Shell, and G. N. Duda. Gait evaluation: a tool to monitor bone healing? *Clin. Biomech.* 20:883–891, 2005.
- ⁴⁹Singare, S., L. Dichen, Y. Liu, W. Zhongying, and J. Wang. The effect of latency on bone lengthening force and bone mineralization: an investigation using strain gauge mounted on internal distractor device. *Biomed. Eng. Online*. 5:18, 2006.
- ⁵⁰Sopakayang, R., and R. De Vita. A mathematical model for creep, relaxation and strain stiffening in parallel-fibered collagen tissues. *Med. Eng. Phys.* 33:1056–1063, 2011.
- ⁵¹Svodoba, Z., L. Bizovska, M. Janura, E. Kubonova, K. Janurova, and N. Vuillerme. Variability of spatial temporal gait parameters and the center of pressure displacements during gait in elderly fallers and nonfallers: a 6-month prospective study. *PLoS ONE*. 12:e0171997, 2017.
- ⁵²Vauhkonen, M., J. Peltonen, E. Karaharju, K. Aalto, and I. Alitalo. Collagen synthesis and mineralization in early phase of distraction bone healing. *Bone Miner.* 10:171–181, 1990.
- ⁵³Waanders, N. A., M. Richards, H. Steen, J. L. Kuhn, S. A. Goldstein, and J. A. Goulet. Evaluation of the mechanical environment during distraction osteogenesis. *Clin. Orthop. Relat. Res.* 349:225–234, 1998.
- ⁵⁴Webb, J., G. Herling, T. Gardner, J. Kenwright, and A. H. R. W. Simpson. Manual assessment of fracture stiffness. *Injury*. 27:319–320, 1996.
- ⁵⁵Wehner, T., M. Steiner, A. Ignatius, and L. Claes. Prediction of the time course of callus stiffness as a function of mechanical parameters in experimental rat fracture healing studies—a numerical study. *PLoS ONE*. 9:e115695, 2014.
- ⁵⁶Wen, H., S. Zhus, C. Li, and Y. Xu. Bone transport versus acute shortening for the management of infected tibial bone defects: a meta-analysis. *BMC Musculoskelet. Disord.* 21:80, 2020.
- ⁵⁷Yin, Q., Z. Sun, S. Gu, Y. Bao, X. Wei, and S. Song. Effectiveness comparison of using bone transport and bone shortening-lengthening for tibial bone and soft tissue defects. *Zhongguo Xiu Fu Chong Jian Wai Ke Za Zhi*. 28:818–822, 2014.

⁵⁸Young, N., F. D. Bell, and A. Anthony. Pediatric pain patterns during Ilizarov treatment of limb length discrepancy and angular deformity. *J. Pediatr. Orthop.* 14:352–357, 1994.

Publisher's Note Springer Nature remains neutral with regard to jurisdictional claims in published maps and institutional affiliations.